Progress In Electromagnetics Research, PIER 23, 277–300, 1999

THE UNIQUENESS PROBLEM OF THE SURFACE INTEGRAL EQUATIONS OF A CONDUCTING BODY IN A LAYERED MEDIUM

A. A. K. Mohsen and A. K. Abdelmageed

Engineering Mathematics and Physics Department
Cairo University
Giza 12211, Egypt

1. INTRODUCTION

Surface integral equations (SIEs) have been widely adopted as efficient tools to handle electromagnetic scattering problems. However, the uniqueness of the solution of these equations is questioned. The electric field integral equation (EFIE) and the magnetic field integral equation (MFIE) are two classes of these SIEs. They yield unique solutions for all the frequency spectrum except at a discrete set of frequencies. This set is related to the interior cavity problem covered by a perfectly conducting surface. At these frequencies, the homogeneous equation yields nontrivial spurious solutions which contaminate the physical solution causing the boundary conditions to be no longer satisfied. Due to the discretization errors encountered in the modeling,

the SIE fails at and in the vicinity of these frequencies.

The diagnosis of the nonuniqueness problem for objects immersed in free space has been located and identified. Several remedies for such case have been suggested, as will be outlined shortly. However, as far as we know, the nonuniqueness problem for an object in a layered medium has not been yet discussed. This is the main object of this article.

For a conducting object in free space, several SIEs and techniques have been proposed to circumvent the shortcoming of the original integral equations. Mitzner [1] proposed a linear combination of the EFIE and MFIE, which is widely known as the combined field integral equation (CFIE). This method was discussed in detail by Mautz and Harrington [2]. A variant of this method is given by Cunefare and Koopmann [3] and is known as coupled Helmholtz integrals (CHI). In CHI, all the field points are restricted to the interior region, thus alleviating the singularity problem. The CFIE method is reliable and yields a unique solution but at the expense of additional computational overhead. Bolomey and Tabbara [4] set up another technique known as the combined source integral equation (CSIE) which was extended later by Mautz and Harrington [5]. In this approach, combined electric and magnetic sources are placed on the surface of the conducting body, and the tangential electric field boundary condition due to these sources is enforced. This approach has the same degree of complexity and computational effort as the CFIE. However, the computed current is not the true one induced on the surface, and additional effort has to be exerted to evaluate it. Yaghjian [6] augmented the EFIE and MFIE with additional constraints in order to enforce the satisfaction of boundary conditions. However, the augmented equations fail to yield the unique solution for the sphere. Schenck [7] overspecified the original SIE system with additional equations that force the interior-region field to vanish. This formulation is known as the combined-Helmholtz integral equation formulation (CHIEF). These additional equations should be satisfied at interior points which do not coincide with nodal surfaces. The resulting overdetermined system is then solved by a least-squares procedure. Although it is argued that the resulting formulation yields a unique solution if at least one point is not located on nodal surfaces [8], this may cause a potential problem as the frequency increases. Waterman [9] developed another approach known as the extended boundary condition method (EBCM). This method was later extended by others

[10, 11]. In this approach, the field points are restricted to the interior region. However, the stability and uniqueness of this approach are questioned [11]. Mohsen [12] used the source simulation technique as an alternative formulation to deal with two-dimensional problems. Monzon and Damaskos [13] proposed an approach called the parasitic body technique to suppress the internal resonances. It assumes the presence of a lossy body inside the resonant geometry, where it interacts only with the resonant fields and attenuates them. However, the need to model such a parasitic body with an additional computational overhead may limit the use of this method. Theoretically, the scattered field of the EFIE is unique. Unfortunately, due to the ill-conditioning of the matrix at and in the vicinity of the resonant frequencies the system solution yields incorrect results. Sarkar and Rao [14] suggested an iterative technique to find the minimum norm solution. Canning [15, 16] used the singular value decomposition (SVD) to isolate and, hence, damp the resonant contribution in the scattered field. Very recently, Mohsen et al. [17] developed a new method called the correction factor technique (CFT). Based on the SVD, the computed current is amended by adding a correction factor term. Canning [18] developed a similar and more general method to account for the surface currents associated with the resonant interior modes.

Despite the immensity of the techniques used to remedy the nonuniqueness problem, one has to resort to some indicator to test the validity of the solution. This is very important, particularly in such cases where no other validation data is available, which is the case of our problem. We choose mainly two indicators: the condition number Cn [19] and the minimum singular value (MSV) [15].

In this work, the nonuniqueness problem of the SIEs of a conducting body in a layered medium is explored. As an application, we will be concerned here with a conducting body of revolution (BOR) in a half-space. Very recently Abdelmageed et al. [20] have developed an electric field integral equation for conducting bodies of revolution (EFIE-BOR) in layered media. Also, Mohsen and Abdelmageed [21] have developed the magnetic field integral equation formulation for the same problem (MFIE-BOR). The uniqueness of both the EFIE-BOR and MFIE-BOR formulations are studied here. The CFIE, CHIEF and CFT techniques are used to treat the nonuniqueness problem. The values of both Cn and MSV are monitored to test the results.

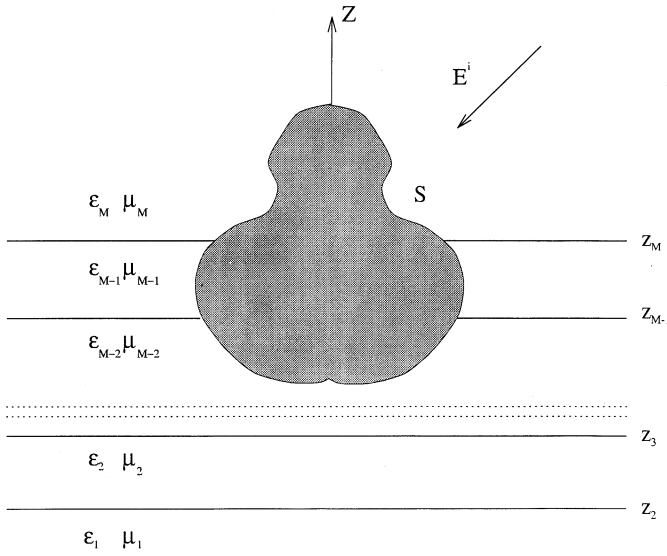

Figure 1. A body of revolution in layered medium.

The paper is organized as follows. In section 2, the uniqueness of the solution of both the EFIE and MFIE of a conducting object in a layered medium is stated. In section 3, the treatment of the nonuniqueness problem is presented. Numerical results are given in section 4. Some concluding remarks are included in section 5.

2. UNIQUENESS OF THE SOLUTION

The EFIE and MFIE formulations of a conducting BOR of surface S in a layered medium (see Fig. 1) have been developed in [20] and [21]. The solution of these integral equations is not unique if the corresponding homogeneous equations have non-trivial solutions. Following the same approach in [2] for the free space case, and in terms of the differential equations governing the electric field $\boldsymbol{E}$, this means that the solution is not unique when there is a non-trivial solution to

$$\nabla \times \nabla \times \boldsymbol{E}(\boldsymbol{r}, \boldsymbol{K}) = k^2(\boldsymbol{r})\boldsymbol{E}(\boldsymbol{r}, \boldsymbol{K}) \quad \text{within S} \tag{1}$$

$$\hat{\boldsymbol{n}} \times \boldsymbol{E}(\boldsymbol{r}, \boldsymbol{K}) = 0 \quad \text{on S} \tag{2}$$

where $\boldsymbol{K}$ and k are the surface current density and the wavenumber, respectively. Also, the continuity of the fields at the interfaces should

be satisfied. Equations similar to (1) and (2) hold for the magnetic field $\boldsymbol{H}$. The wavenumber k depends on $\boldsymbol{r}$ to denote its variation from one layer to another. The layers are assumed to be homogeneous and isotropic. These equations represent the resonant modes of a cavity resonator covered by a perfect conductor S. The structure of the cavity has the same media parameters as the surrounding media. Thus, if the object is totally confined to one layer of wavenumber k, then the resonant modes would be the same as those of an object immersed in a space of wavenumber k. Also, like free space both $\boldsymbol{E}$ and $\boldsymbol{H}$ field equations have the same set of modes. When the object is penetrating the interface between two layers, the location of the resonant modes is no longer an easy task. This is even so for a simple structure like a sphere. The modes depend on the depth of penetration. Unlike the free-space case, $\boldsymbol{E}$ and $\boldsymbol{H}$ field equations have different sets of modes. All these arguments will be clarified below.

3. TREATMENT OF THE NONUNIQUENESS PROBLEM

A survey of many techniques proposed to tackle the nonuniqueness problem has been presented in the introduction. We discuss here three of these techniques: the CFIE, CHIEF and CFT methods. The CFIE method uses a linear combination of both the EFIE and MFIE. Although the CFIE method is complicated in nature, it is a very reliable technique when used in free space. The CFIE is given in operator form as

$$\left[H^i\right] + \frac{\alpha}{\eta_n}\left[E^i\right] = \left\{[Y] + \frac{\alpha}{\eta_n}[Z]\right\}[I] \tag{3}$$

$[Z]$ and $[Y]$ are the equivalent matrices of the EFIE and MFIE formulations, respectively. $\left[E^i\right]$ and $\left[H^i\right]$ are their corresponding excitation vectors, and $[I]$ is the unknown current vector to be determined. The coupling factor α is a real positive number and it is usually selected in the range $0 < \alpha < 1$ [2] for free space. When the body is confined to one layer, $\eta_n = \sqrt{\mu_n/\epsilon_n}$ is the intrinsic impedance of this layer. Otherwise, there is an ambiguity in determining its value. In such a case, we set its value to the intrinsic impedance of free space. In free space, α is chosen in such a way as to minimize the mean error. This error is usually obtained by comparing the computed results with the available exact solutions for some simple shapes like a sphere. The usual selected value for free space is $\alpha = 0.2$. However, Mautz and Harrington [2] argued that the error is small for any value of α from

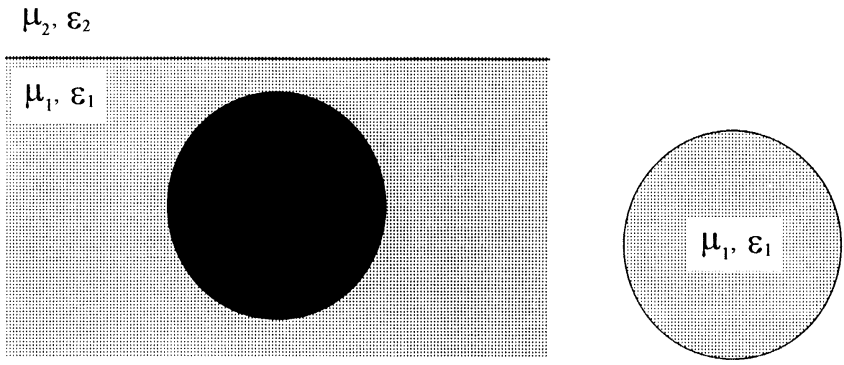

(a) A buried sphere. (b) The corresponding cavity.

Figure 2. A conducting sphere present in a half-space and the corresponding cavity.

0.2 to 1. In a layered medium, the situation is different as we do not have an exact solution for any shape. Nevertheless, the optimum value may be deduced by observing Cn or MSV as α changes.

For the CHIEF method, the equivalent $N \times N$ system of equations of the original formulation, is augmented by additional M equations. The field points of these equations are restricted to the interior region. The resulting $(N + M) \times N$ overdetermined system is solved by a least-squares procedure.

Based on SVD, the CFT method enforces the interior field to vanish [17]. At resonant modes, a correction factor term is added to the computed current $\boldsymbol{K}$. Hence, the corrected current $\boldsymbol{K}_c$ is expressed as

$$\boldsymbol{K}_c = \boldsymbol{K} + A\boldsymbol{K}_r \tag{4}$$

where A is an unknown complex factor to be determined. $\boldsymbol{K}_r$ is the normalized resonant mode current. Using the power method [16], it is computed as the largest eigenvector of $\left[[Z]^H[Z]\right]^{-1}\left(\left[[Y]^H[Y]\right]^{-1}\right)$, where $[Z]([Y])$ is the impedance (admittance) matrix generated by the moment method. The subscript $\boldsymbol{H}$ denotes taking the Hermitian conjugate. A is computed by enforcing the interior electric (magnetic) field $\boldsymbol{E}(\boldsymbol{H})$ to vanish, hence

$$\mathcal{F}(\boldsymbol{K}_c) + \mathcal{F}^i = 0 \tag{5}$$

where $\mathcal{F}$ stands for either the scattered electric or magnetic fields. Using (4), $\mathcal{F}(\boldsymbol{K}_c)$ may be expressed as

$$\mathcal{F}(\boldsymbol{K}_c) = \mathcal{F}(\boldsymbol{K}) + A\mathcal{F}(\boldsymbol{K}_r) \tag{6}$$

Satisfying (5) and (6) at a selected interior point results in obtaining A and hence $\boldsymbol{K}_c$. This point should be away from any nodal surface. In this approach, the authors in [17] considered only one resonance mode. To take other modes into consideration, Canning [18] developed a more general approach to compute the corrected current.

4. NUMERICAL RESULTS

The results of the CFIE, CHIEF and CFT methods for a BOR in a half-space excited by an incident plane wave will be presented. Both the CHIEF and CFT method are used to correct the EFIE. The following three cases will be studied here:

- A conducting sphere above and below the interface.
- A conducting sphere penetrating the interface.
- A conducting pillbox penetrating the interface.

4.1 A Conducting Sphere above and below the Interface

A conducting sphere of radius a buried in a homogeneous medium (μ_1, ϵ_1) is illustrated in Fig. 2a. Its corresponding cavity resonator enclosing the same medium (μ_1, ϵ_1) is shown in Fig. 2b. Tabulation of the resonant frequencies for a spherical cavity enclosing free space is given in [22, p. 270]. For the considered case here, these values should be divided by $\sqrt{\mu_1\epsilon_1}$. On the other hand, for a sphere above the interface the resonant frequencies are given by these tabulated values divided by $\sqrt{\mu_2\epsilon_2}$.

It is conceivable that the choice of α is important for the CFIE technique to work well. To determine the best value, Cn and MSV are monitored as α changes. At the optimal value, Cn attains its minimum and MSV reaches its maximum.

In Figs. 3 and 4, MSV and Cn for the CFIE technique are shown versus α for a sphere above and below the interface, respectively. The results are computed for $\epsilon_1 = 2, 6, 10$ and 16, and $\epsilon_2 = 1$. In Fig. 3, the sphere radius is $k_2 a = 2.744$ corresponding to the first resonant frequency for a spherical cavity in a space of wavenumber k_2, while in Fig. 4, the sphere radius is $k_1 a = 2.744$. In both figures, MSV reaches its maximum at $\alpha = 0.5 \sim 0.6$ and Cn attains its minimum

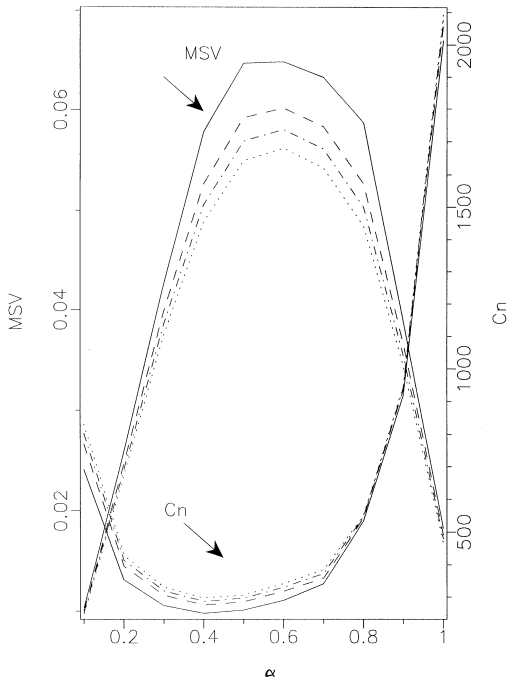

Figure 3. MSV and Cn of CFIE as functions of α for a sphere above the interface with the parameters: $\epsilon_2 = 1.0$, $\theta^i = 0.0°$, $k_2 a = 2.744$ and $d = 0.2\lambda_o$. $\epsilon_1 = 2$: ——, $\epsilon_1 = 6$: − − −, $\epsilon_1 = 10$: − · −·, $\epsilon_1 = 16$: ..... .

at $\alpha = 0.4$. These values are figures of merit for the success of the results. There is no contradiction here between these values, as the solution is usually stable for some range of α. We have tried other extensive results, and the same argument is still valid irrespective of the resonant frequency or how far the object is from the interface.

To compare the performance of the CFIE and CFT techniques with that of the EFIE and MFIE at the resonant frequencies, the current distributions for two different cases are shown in Figs. 5–8. For these cases the sphere radius is given by $k_2 a = 2.744$ and $k_1 a = 2.744$, respectively. The current distribution is plotted versus the normalized parameter s, which runs from $s = 0(\ell_o)$ to $s = 1(\ell_f)$, where (ℓ_o) and (ℓ_f) are the starting and ending tips of the generating arc ℓ. The number of segments NS is set to 41 and the number of interior points for the CHIEF technique is 7. In the first case, the sphere is in the upper space with $d = 0.2\lambda_o$ while in the other case it is in the lower

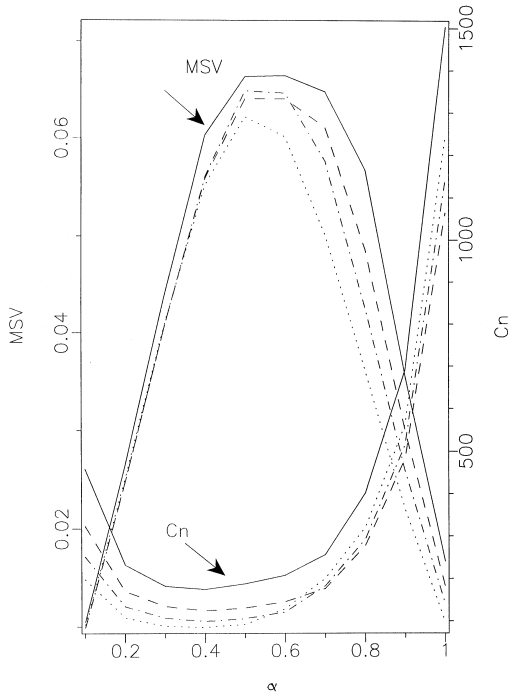

Figure 4. MSV and Cn of CFIE as functions of α for a sphere below the interface with the parameters: $\epsilon_2 = 1.0$, $\theta^i = 0.0°$, $k_1 a = 2.744$ and $d = -0.8\lambda_o$. $\epsilon_1 = 2$: ——, $\epsilon_1 = 6$: − − −, $\epsilon_1 = 10$: − · −·, $\epsilon_1 = 16$: ..... .

space with $d = -0.4\lambda_o$ where d is the distance from the interface to the lower tip of the sphere. The $+(-)$ sign means that the lower tip is in the upper (lower) half-space. The dielectric constant of the lower space is 10. For the CFIE technique, α is chosen equal to 0.6.

For the CHIEF technique, the interior points are chosen to lie on a concentric sphere of radius $a/2$. For the CFT technique, the interior point is chosen at $(r, \theta) = (a/2, 0)$. The figures show that the CFIE, CHIEF and CFT results are in good agreement. The results of the EFIE and MFIE techniques are also included for comparison. To test the performance of the different SIEs MSV, Cn and CPU time for the two cases are shown in Tables 1–2. The CFT has a self-accuracy test; so no test is required here. At resonant frequencies, Cn reaches a high value; while MSV attains a low value. This is evident by observing the results of the EFIE and MFIE. The effect of the CFIE and CHIEF on both Cn and MSV is quite clear. Both the Cn and MSV

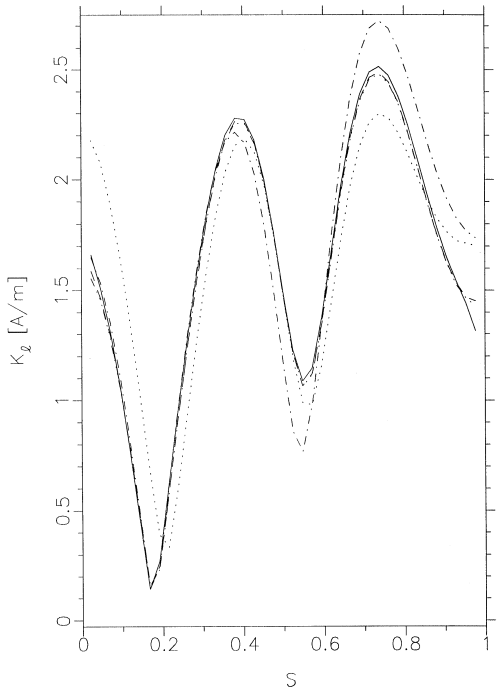

Figure 5. Magnitude of K_ℓ on a metallic sphere present in the upper space with the parameters: $\epsilon_1 = 10.0$, $\epsilon_2 = 1.0$, $\theta^i = 0.0°$, $k_2 a = 2.744$ and $d = 0.2\lambda_o$. EFIE: ....., MFIE: $- \cdot -\cdot$, CFIE: ——, CFT: $- \cdots$, CHIEF: $- - -$.

are significantly improved. This indicates that Cn and MSV can be used as efficient indicators for both CFIE and CHIEF. A point which deserves attention here is the range of Cn and MSV for EFIE and MFIE at the resonant frequencies. Although the matrices of both formulations become ill-conditioned at these frequencies, the range of Cn and MSV is different. Cn (MSV) is much higher (lower) for the EFIE than MFIE. This shows that the use of Cn and MSV as indicators is formulation-dependent.

Observing the CPU time given in Tables 1–2, we notice that the time is nearly doubled for the CFIE technique compared with the CHIEF and CFT techniques. The CFT seems the most efficient method as it requires less Memory Storage and less CPU time. It causes less than 8% increase in CPU time compared with 25% and more than 100% for CHIEF and CFIE, respectively.

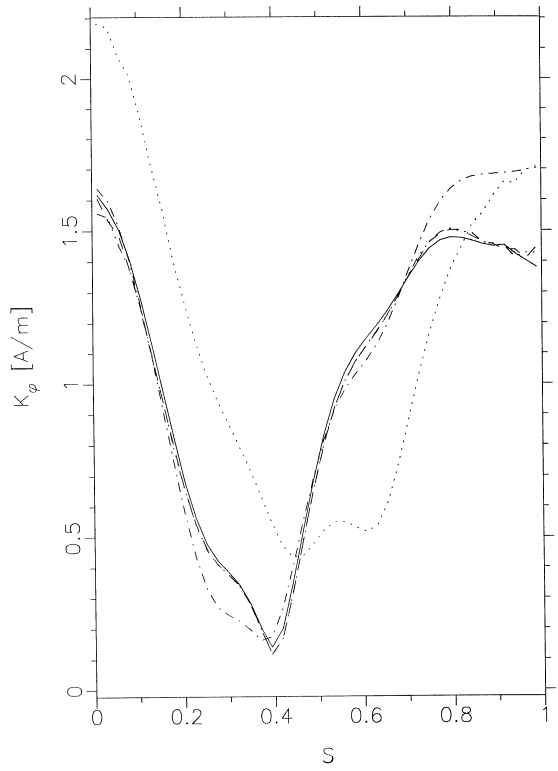

Figure 6. Magnitude of K_φ on a metallic sphere present in the upper space with the parameters: $\epsilon_1 = 10.0,\ \epsilon_2 = 1.0,\ \theta^i = 0.0°,\ k_2 a = 2.744$ and $d = 0.2\lambda_o$. EFIE: ....., MFIE: $- \cdot -\cdot$, CFIE: ——, CFT: $- \cdots$, CHIEF: $- - -$.

SIE	Cn	MSV	CPU Time in Sec.
EFIE	67357	0.00029	27
MFIE	4505	0.00077	35
CFIE	601	0.029	62
CHIEF	842	0.040	34
CFT			29

Table 1. Performance of SIEs for a sphere in the upper space with $k_2 a = 2.744,\ d = 0.2\lambda_o,\ \theta^i = 0.0°,\ \epsilon_1 = 10$ and $\epsilon_2 = 1$.

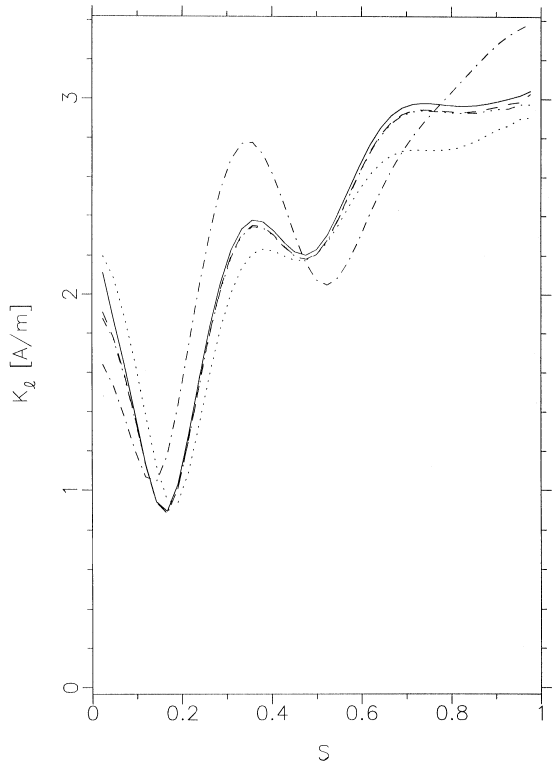

Figure 7. Magnitude of K_ℓ on a metallic sphere present in the lower space with the parameters: $\epsilon_1 = 10.0$, $\epsilon_2 = 1.0$, $\theta^i = 0.0°$, $k_1 a = 2.744$ and $d = -0.4\lambda_o$. EFIE: ....., MFIE: $-\cdot-\cdot$, CFIE: ——, CFT: $-\cdots$, CHIEF: $---$.

SIE	Cn	MSV	CPU Time in Sec.
EFIE	39287	0.000077	28
MFIE	2332	0.00077	34
CFIE	328	0.028	52
CHIEF	902	0.00473	35
CFT			30

Table 2. Performance of SIEs for a sphere in the lower space with $k_1 a = 2.744$, $d = -0.4\lambda_o$, $\theta^i = 0.0°$, $\epsilon_1 = 10$ and $\epsilon_2 = 1$.

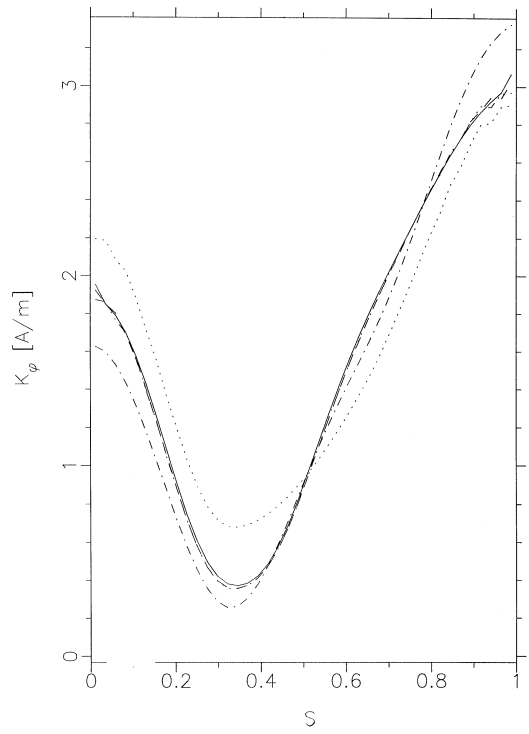

Figure 8. Magnitude of K_φ on a metallic sphere present in the lower space with the parameters: $\epsilon_1 = 10.0$, $\epsilon_2 = 1.0$, $\theta^i = 0.0°$, $k_1 a = 2.744$ and $d = -0.4\lambda_o$. EFIE: ....., MFIE: $-\cdot-\cdot$, CFIE: ——, CFT: $-\cdots$, CHIEF: $- - -$.

4.2 A Conducting Sphere Penetrating the Interface

For a penetrating sphere, there is no explicit formula to detect the resonant frequencies. One way to detect these frequencies is the numerical approach. Fig. 9 shows the MSV and Cn versus $k_o a$ of a half-buried sphere for EFIE. $\epsilon_1 = 10$, $\epsilon_2 = 1$ and $\theta^i = 0.0°$. Although both the EFIE and MFIE yield the same resonant frequencies when the sphere is embedded in one layer, the matter seems different here. For a penetrating sphere, the EFIE and MFIE have different frequencies. In Table 3, the first frequency of a half-buried metallic sphere for $m = 1$ is shown for $\epsilon_1 = 2, 6, 10$ and 16. At these frequencies one formulation succeeds and the other fails. The use of the CFIE may seem inappropriate in this case as one can switch directly to the

successful formulation. It is hard to determine this for any arbitrary object without deliberate investigation. In this context, the CHIEF and CFT may seem more appropriate.

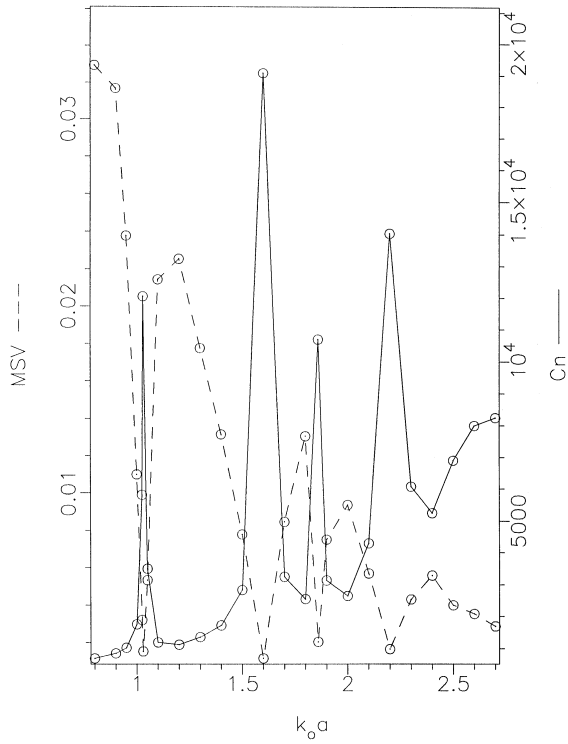

Figure 9. MSV and Cn of EFIE versus $k_o a$ for a half-buried metallic sphere with the parameters: $\epsilon_1 = 10.0,\ \epsilon_2 = 1.0,\ \theta^i = 0.0°$.

Formulation	Resonant frequencies given in terms of $k_o a$			
	$\epsilon_1 = 2$	$\epsilon_1 = 6$	$\epsilon_1 = 10$	$\epsilon_1 = 16$
EFIE	2.176	1.325	1.035	0.822
MFIE	2.283	1.534	1.217	0.973

Table 3. The first resonant frequency of a half-buried metallic sphere for EFIE and MFIE with $\theta^i = 0.0°,\ \epsilon_2 = 1$.

The currents of a half-buried sphere of radius $k_o a = 1.035$ are shown in Figs. 10 and 11 for $\theta^i = 0.0^\circ$, $\epsilon_1 = 10$ and $\epsilon_2 = 1$. At these values, the EFIE fails. As evident from the figures, the MFIE, CHIEF and CFT agree well.

4.3 A Conducting Pillbox Penetrating the Interface

In Fig. 12a, the problem of a conducting pillbox penetrating the interface is depicted. The corresponding cavity is shown in Fig. 12b. The EFIE fails at the resonant frequencies of an electric cavity whose structure is depicted in Fig. 12b. On the other hand, the MFIE fails at the resonant frequencies of a magnetic cavity having the same structure of Fig. 12b. The resonant frequencies of the electric and magnetic cavities are given in the Appendix. They are given the notation TE_{mng} and TM_{mng} for the transverse electric and transverse magnetic modes, respectively. It is evident that the MFIE has a different set of modes from that of EFIE. This is contrary to the free space case where both the EFIE and MFIE have the same set of modes.

The first four EFIE resonant frequencies of $m = 1$ for $\epsilon_1 = 10$, $\epsilon_2 = 1$, $L/a = 2.0$ and $d/a = 0.5$, 1.0 and 1.5 are given in Table 4. Using the EFIE, the MSV and Cn versus $k_o a$ for $d/a = 1.0$ and $d/a = 1.5$ are illustrated in Figs. 13–14, respectively. As evident at the resonant frequencies both MSV and Cn efficiently detect the failure of EFIE. The currents for $d/a = 1.0$ at the first resonant frequency $k_o a = 0.9174$ are shown in Figs. 15, 16. At this value the EFIE fails. Results of the EFIE, MFIE, CHIEF techniques and CFT are presented. A good agreement between the MFIE, CHIEF and CFT is achieved.

5. CONCLUSION

The uniqueness of the EFIE and MFIE for a conducting object in a layered medium is presented. A case study of a BOR in a half-space is studied. The CFIE, CHIEF and CFT are used to treat the failure of the solution at resonant frequencies. It is shown that the EFIE and MFIE fail at the same resonant frequencies when the object is confined to one layer. For this case, the coupling factor α of the CFIE is found to yield the best results in the range of $\alpha = 0.4 \sim 0.6$. This was determined by observing the minimum singular value MSV and condition number Cn. On the other hand, when the object is penetrating the interface the EFIE and MFIE fail at different sets of resonant frequencies. These

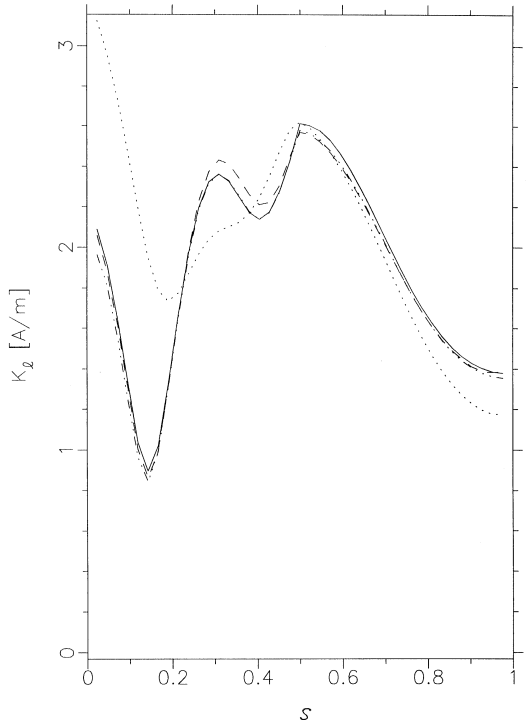

Figure 10. Magnitude of K_ℓ on a half-buried metallic sphere with the parameters: $\epsilon_1 = 10.0,\ \epsilon_2 = 1.0,\ \theta^i = 0.0°, k_o a = 1.035$. EFIE: ....., MFIE: ——, CFT: $-\cdots$, CHIEF: $- - -$.

Rfs for $m = 1$	$d/a = 0.5$		$d/a = 1.0$		$d/a = 1.5$	
	Rf	order	Rf	order	Rf	order
1	1.3381	TE_{111}	0.9147	TE_{111}	0.7904	TE_{111}
2	1.5337	TM_{111}	1.3046	TM_{111}	1.2578	TE_{112}
3	2.2543	TE_{121}	1.6698	TE_{112}	1.5546	TM_{111}
4	2.4191	TM_{121}	1.8830	TE_{121}	1.7856	TE_{121}

Table 4. Resonant frequencies (Rf) of EFIE, given in terms of $k_o a$, of a pillbox penetrating the interface for $\theta^i = 0.0°,\ \epsilon_1 = 10,\ \epsilon_2 = 1$ and $L/a = 2.0$.

frequencies are located analytically for a penetrating pillbox. However, one can not distinguish between these frequencies for a general object without a prior analysis. In this context, the CHIEF and CFT may seem more appropriate than the CFIE. A comparison between the CFIE, CHIEF and CFT have shown that CFT is the most efficient technique. MSV and Cn have been used to test the validation of the solution. They are found to be good indicators for the failure or success of the formulation. However, the range of Cn and MSV is formulation-dependent.

APPENDIX

In Fig. 17, a partially filled circular cylindrical cavity is shown. a and L are, respectively, the radius and length of the cavity. For $0 < z < d$, it is filled with a dielectric of (μ_1, ϵ_1) while for $d < z < L$, it is filled with a dielectric of (μ_2, ϵ_2). For the electric cavity, the solution must satisfy the condition of a zero tangential $\boldsymbol{E}$ at $\rho = a$, $z = 0$ and $z = L$. For TM modes, a suitable solution is given by the magnetic vector potential $\boldsymbol{A} = \Psi^{TM}\hat{\boldsymbol{u}}_z$ where Ψ^{TM} is expressed as

$$\Psi^{TM}_{mnq} = AJ_m\left(X_{mn}\frac{\rho}{a}\right)e^{jm\varphi}\cos[k_{z1}z]; \qquad 0 < z < d \tag{7}$$

$$\Psi^{TM}_{mnq} = BJ_m\left(X_{mn}\frac{\rho}{a}\right)e^{jm\varphi}\cos[k_{z2}(L-z)]; \qquad d < z < L \tag{8}$$

where

$$k_{z1a} = \sqrt{(k_1 a)^2 - X^2_{mn}} \tag{9}$$

$$k_{z2a} = \sqrt{(k_2 a)^2 - X^2_{mn}} \tag{10}$$

$m = 0, 1, 2, \cdots$, $n = 1, 2, 3, \cdots$ and X_{mn} is the nth zero of $J_m(x) = 0$. A tabulation of these zeros is given in [22, pp. 205]. The meaning of the subscript $q = 1, 2, 3, \cdots$ will be clarified below. To determine the constants A and B, we should satisfy the boundary conditions at $z = d$. These conditions require the continuity of E_ρ, E_φ, H_ρ and H_φ. Satisfying these conditions, one can deduce that

$$\frac{k_{z1}a}{\epsilon_1}\tan\left[k_{z1}a\left(\frac{d}{a}\right)\right] = -\frac{k_{z2}a}{\epsilon_2}\tan\left[k_{z2}a\left(\frac{L}{a} - \frac{d}{a}\right)\right] \tag{11}$$

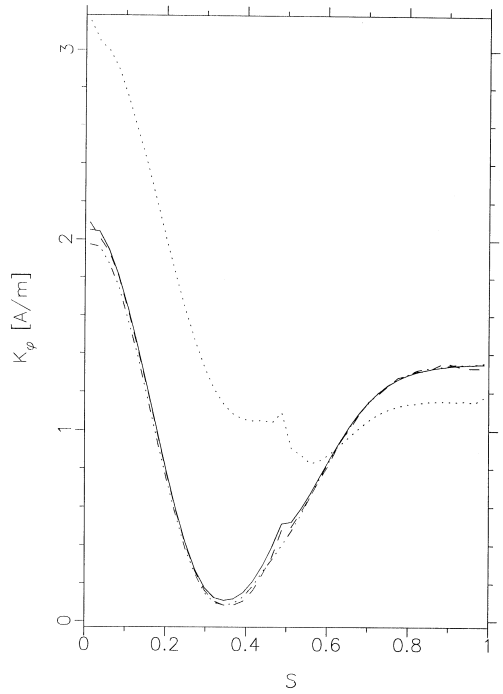

Figure 11. Magnitude of K_φ on a half-buried metallic sphere with the parameters: $\epsilon_1 = 10.0,\ \epsilon_2 = 1.0,\ \theta^i = 0.0°, k_o a = 1.035$. EFIE: ....., MFIE: ——, CFT: $- \cdots$, CHIEF: $- - -$.

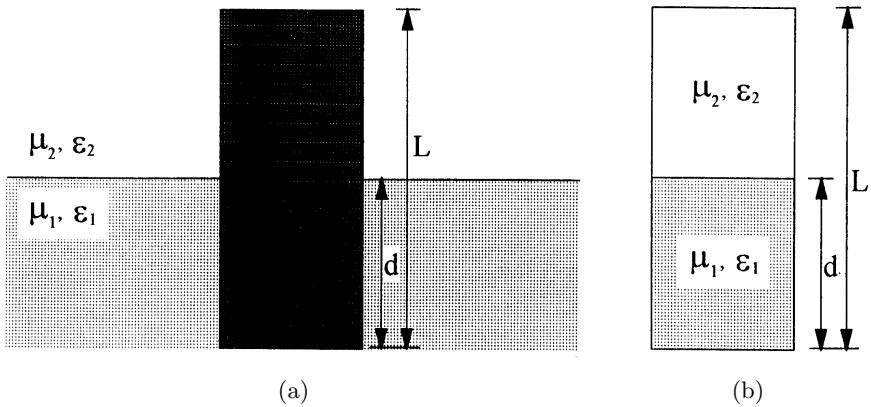

Figure 12. A metallic pillbox penetrating the interface and the corresponding cavity: (a) A penetrating pillbox (b) The corresponding cavity.

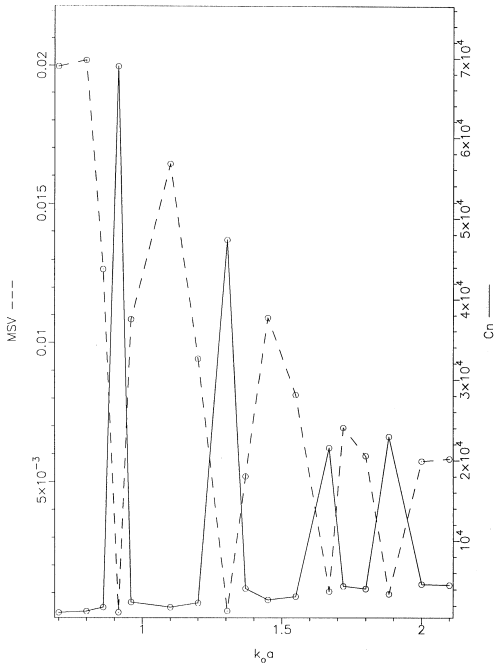

Figure 13. MSV and Cn of EFIE versus $K_o a$ for a metallic pill-box penetrating the interface with the parameters: $\epsilon_1 = 10.0$, $\epsilon_2 = 1.0$, $\theta^i = 0.0°, L/a = 2.0$ and $d/a = 1.0$.

Solution of the transcendental equation (11) yields different values for $k_o a$ for a certain X_{mn}. The order of these values is given by the subscript q of the mode TM_{mnq}.

Similarly for TE modes, we can deduce that

$$\frac{k_{z1}a}{\mu_1} \cot\left[k_{z1}a\left(\frac{d}{a}\right)\right] = -\frac{k_{z2}a}{\mu_2} \cot\left[k_{z2}a\left(\frac{L}{a} - \frac{d}{a}\right)\right] \tag{12}$$

where

$$k_{z1}a = \sqrt{(k_1 a)^2 - {X'_{mn}}^2} \tag{13}$$

$$k_{z2}a = \sqrt{(k_2 a)^2 - {X'_{mn}}^2} \tag{14}$$

and X'_{mn} is the nth zero of $J'_m(x) = 0$. A tabulation of these zeros is given in [22, pp. 205]. Solution of the transcendental equation (12)

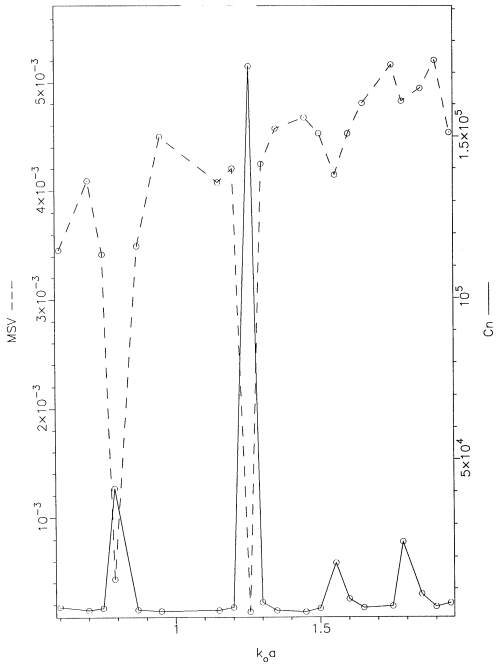

Figure 14. MSV and Cn of EFIE versus $k_o a$ for a metallic pillbox penetrating the interface with the parameters: $\epsilon_1 = 10.0,\ \epsilon_2 = 1.0,\ \theta^i = 0.0^\circ, L/a = 2.0$ and $d/a = 1.5$.

yields different values for $k_o a$ for a certain X'_{mn}. The order of these values is given by the subscript q of the mode TE_{mnq}.

For the magnetic cavity, the tangential magnetic field vanishes at the cavity walls. Therefore, the solution must satisfy the condition of a zero tangential $\boldsymbol{H}$ at $\rho = a,\ z = 0$ and $z = L$. Hence, the magnetic cavity problem is the dual of the electric cavity problem. The TM and TE solutions are given by Ψ^{TE}_{mnq} and Ψ^{TM}_{mnq}, respectively. Satisfying the boundary conditions for TM fields at $z = d$ yields

$$\frac{k_{z1}a}{\epsilon_1}\cot\left[k_{z1}a\left(\frac{d}{a}\right)\right] = -\frac{k_{z2}a}{\epsilon_2}\cot\left[k_{z2}a\left(\frac{L}{a}-\frac{d}{a}\right)\right] \tag{15}$$

and for TE fields yields

$$\frac{k_{z1}a}{\mu_1}\tan\left[k_{z1}a\left(\frac{d}{a}\right)\right] = -\frac{k_{z2}a}{\mu_2}\tan\left[k_{z2}a\left(\frac{L}{a}-\frac{d}{a}\right)\right] \tag{16}$$

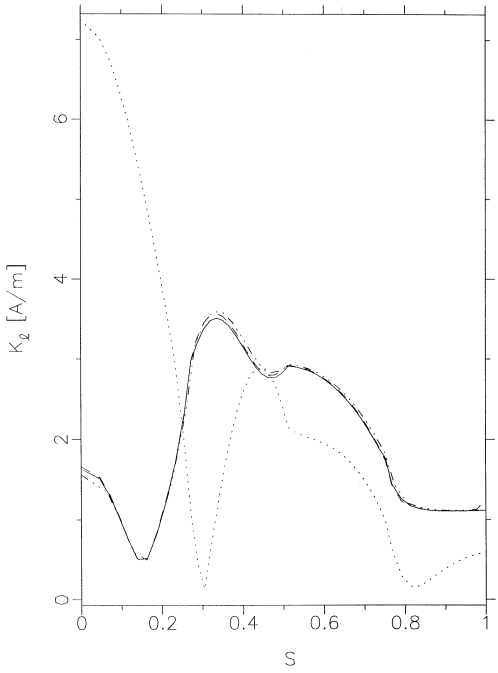

Figure 15. Magnitude of K_ℓ on a half-buried metallic pillbox with the parameters: $\epsilon_1 = 10.0,\ \epsilon_2 = 1.0,\ \theta^i = 0.0°, L/a = 2.0$ and $k_o a = 0.9147$. EFIE: ....., MFIE: ——, CFT: $- \cdots$, CHIEF: $- - -$.

Solution of the transcendental equations (15) and (16) yields different values for $k_o a$ for a certain X'_{mn} and X_{mn}, respectively. The order of these values is given by the subscript q of the modes TM_{mnq} and TE_{mnq}.

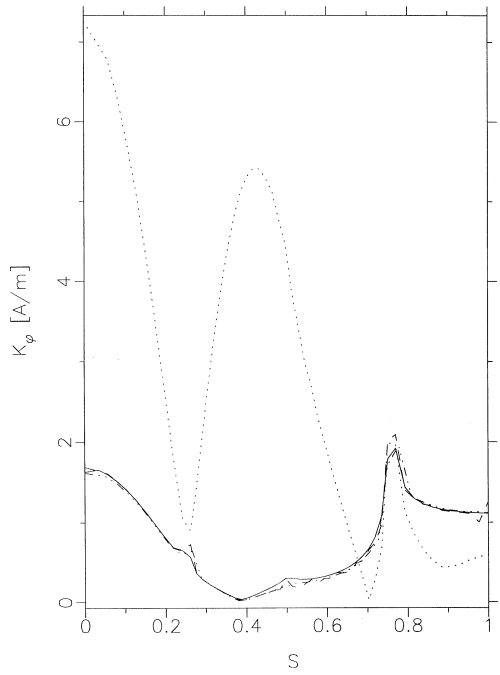

Figure 16. Magnitude of K_φ on a half-buried metallic pillbox with the parameters: $\epsilon_1 = 10.0,\ \epsilon_2 = 1.0,\ \theta^i = 0.0°, L/a = 2.0$ and $k_o a = 0.9147$. EFIE: ....., MFIE: ——, CFT: $-\cdots$, CHIEF: $---$.

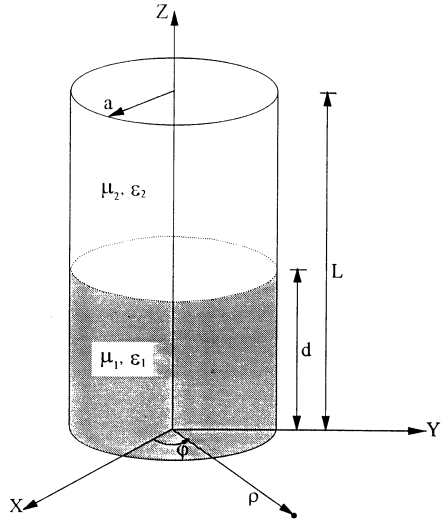

Figure 17. Partially filled circular cylindrical cavity.

REFERENCES

1. Mitzner, K. M., "Numerical solution of the exterior scattering problem at eigen frequencies of the interior problem," *Digest URSI Rad. Sci. Meeting,* 75, Boston, MA, 1968.
2. Mautz, J. R., and R. F. Harrington, "H-field, E-field and combined field solutions for conducting bodies of revolutions," *Arch. Elek. Übertragung.,* Vol. 32, 157–164, 1978.
3. Cunefare, K. A., and G. Koopmann, "A boundary element method for acoustic radiation valid for all wavenumbers," *J. Acoust. Soc. Am.,* Vol. 85, 39–48, 1989.
4. Bolomey, J. C., and W. Tabbara, "Numerical aspects on coupling between complementary boundary value problems," *IEEE Trans. Antennas Propagat.,* Vol. 21, 356–363, 1973.
5. Mautz, J. R., and R. F. Harrington, "A combined-source solution for radiation and scattering from a perfectly conducting body," *IEEE Trans. Antennas Propagat.,* Vol. 27, 445–454, 1979.
6. Yaghjian, A. D., "Augmented electric- and magnetic-field integral equations," *Radio Sci.,* Vol. 16, 987–1001, 1981.
7. Schenck, H. A., "Improved integral formulation for acoustic radiation problems," *J. Acoust. Soc. Am.,* Vol. 44, 41–58, 1968.
8. Seybert, A. F., and T. K. Rengarajan, "The use of CHIEF to obtain unique solutions for acoustic radiation using boundary integral equations," *J. Acoust. Soc. Am.,* Vol. 81, 1299–1306, 1987.
9. Waterman, P. C., "Matrix formulation of electromagnetic scattering," *Proc. IEEE,* Vol. 53, 805–812, 1965.
10. Al-Badwaihy, K. A., and J. L. Yen, "Extended boundary condition integral equations for perfectly conducting bodies: uniqueness and formulation," *IEEE Trans. Antennas Propagat.,* Vol. 23, 1545–1552, 1975.
11. Toyoda, I., M. Matsuhara, and N. Kumagai, "Extended integral equation formulation for scattering problems from a cylindrical scatterer," *IEEE Trans. Antennas Propagat.,* Vol. 36, 1580–1586, 1988.
12. Mohsen, A., "The source simulation technique for exterior problems in acoustics," *Z. Angew Math. Phys.,* Vol. 43, 401–404, 1992.
13. Monzon, J. C., and N. J. Damaskos, "A scheme for eliminating internal resonances: the parasitic body technique," *IEEE Trans. Antennas Propagat.,* Vol. 42, 1089–1096, 1994.
14. Sarkar, T. K., and S. M. Rao, "A simple technique for solving E-field integral equations for conducting bodies at internal resonances," *IEEE Trans. Antennas Propagat.,* Vol. 30, 1250–1257, 1982.

15. Canning, F. X., "Singular value decomposition of integral equations of EM and applications to the cavity resonance problem," *IEEE Trans. Antennas Propagat.,* Vol. 37, 1156–1163, 1989.
16. Canning, F. X., "Protecting EFIE-based scattering computations from effects of interior resonances," *IEEE Trans. Antennas Propagat.,* Vol. 39, 1545–1552, 1991.
17. Mohsen, A., A. Helaly, and H. M. Fahmy, "The corrected induced surface current for arbitrary conducting objects at resonance frequencies," *IEEE Trans. Antennas Propagat.,* Vol. 43, 448–452, 1995.
18. Canning, F. X., "Robust use of supplementary conditions for moment method solutions near internal resonances," *IEEE Trans. Antennas Propagat.,* Vol. 43, 264–269, 1995.
19. Mittra, R., and C. A. Klein, "Stability and convergence of moment method solutions," in *Numerical and Asymptotic Techniques in Electromagnetics,* R. Mittra (ed.), Springer-Verlag, New York, 1975.
20. Abdelmageed, A. K., K. A. Michalski, and A. W. Glisson, "Analysis of EM scattering by conducting bodies of revolution in layered media using the discrete complex image method," in *Digest IEEE AP-S Int. Symp.,* 402–405, Newport, Ca, 1995.
21. Mohsen, A., and A. K. Abdelmageed, "Magnetic field integral equation for electromagnetic scattering by conducting bodies of revolution in layered media," *J. Electromagn. Waves Appl.,* submitted for publication.
22. Harrington, R. F., *Time-Harmonic Electromagnetic Fields,* McGraw-Hill, New York, 1961.